

Development of a High Bandwidth, High Power Linear Amplifier for a Precision Fast Tool Servo System

S. Rakuff¹, J. Cuttino¹, D. Schinstock²

¹Dept. of Mechanical Engineering, The University of North Carolina at Charlotte, Charlotte, NC 28223

²Dept. of Mechanical Engineering, Tulsa University, Tulsa, OK 74104

1. Introduction

A “long-range” fast tool servo (FTS) has been developed at UNC-Charlotte that is currently able to deliver ± 1 mm linear motions at frequencies as high as 50 Hz. To date the accuracy is $0.1 \mu\text{m}$ for a $\pm 250 \mu\text{m}$ sinusoidal oscillatory motion at 20Hz. The FTS consists of a DSP-system, a voice coil driven flexure carrying the diamond cutting tool, and a laser interferometer, which is used for position feedback. A PID algorithm running on the DSP card is used for position control. The controller signal is amplified with a high performance analog amplifier to drive the voice coil.

The high power output and bandwidth requirements of the amplifier mean that it must be a carefully designed, integral part of the FTS system. The amplifier in this paper features the APEX PA03 linear operational amplifier. The paper describes the design techniques applied during development of the amplifier circuit and points out how classical control techniques can be used.

2. Design objective

The amplifier is designed to operate in a frequency span from DC up to 50Hz. This distinguishes the amplifier from commercially available audio amplifiers, which are typically designed as band pass filters. A requirement for the FTS was to be able to hold the flexure at a commanded fixed position with a constant force, which corresponds to a nominally constant current through the voice coil. However, typical signal frequencies will lie around 40 Hz, which is close to the fundamental frequency of the flexure. Operating the system close to its natural frequency helps to conserve power but is also harder to control.

Because of the low pass filter characteristics of the amplifier, design techniques from classical controls may be optimally applied in the design process. In its simplest form, the voice coil can be modeled as a resistor in series with an inductance. This gives a transfer function between the load current and the load voltage of

$$TF = \frac{I_L}{V} = \frac{1}{Ls + R_L} \quad (1)$$

where $L=2.5\text{mH} \pm 30\%$ and $R_L=2.4\Omega \pm 12.5\%$ taken from the data sheet of the voice coil. Figure 1 shows the Bode plots of the voice coil for L and R varying within their uncertainties. The -3dB bandwidth is only about 1000rad/s (159Hz), which would also be the bandwidth of an open loop amplifier configuration. The bandwidth can be increased if a properly designed controller and feedback network is implemented.

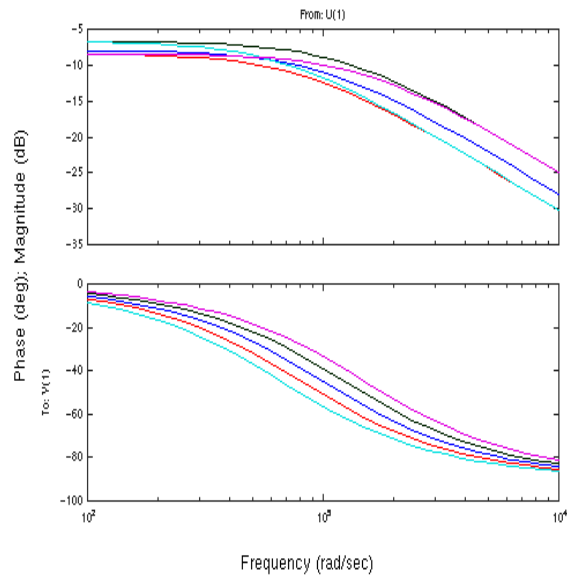


Figure 1: Frequency response of the voice coil

3. Voltage controlled current sources

The amplifier is designed as a voltage controlled current source, or VCCS. The amplifier converts the position command voltage from the DSP card into a current flow I_L through the voice coil to move the flexure. The voltage to current conversion factor is set to 2.2A/V. The voice coil is assumed to behave like an ideal actuator having a linear relationship between the current and the output force. The force constant is

$$K_f = 21.3 \frac{N}{A} \quad (2)$$

To generate a sinusoid force with an amplitude of 100N at a frequency of $f=50\text{Hz}$ ($\omega=314.2\text{rad/s}$), the required current amplitude I_L is 4.68A. From figure 2 it can be seen that the voltage across the load impedance R_L and L_L is the difference between v_L and v_S . If the feedback resistor R_f is large compared to the sense resistor R_s , then it can be assumed that all current flowing through the load will eventually flow to ground, so that i_L is approximately equal to i_s . The voltage drop across the load can then be written as

$$v_L \cong L \frac{di_L}{dt} + (R_L + R_s) i_L \quad (3)$$

where

$$\frac{d}{dt} i_L(t) = -\omega I_L \sin(\omega t) \quad (4)$$

The magnitude of di_L/dt is maximized at times $t = 0, \pi/\omega, 2\pi/\omega$, and so forth. The magnitude of the voltage is about 12V. As shown in figure 3, the voltage will lead the current by a phase angle \mathbf{f} .

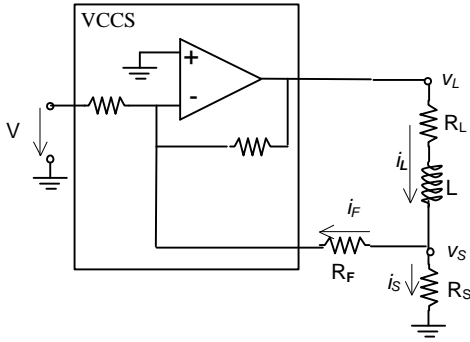


Figure 2: Voltage controlled current source (VCCS)

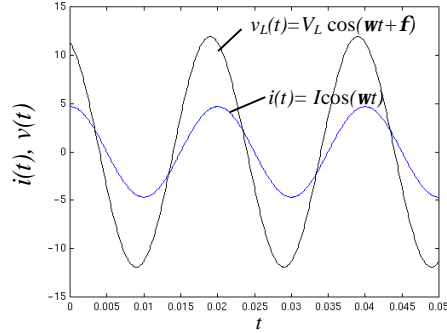


Figure 3: Current voltage relationship

If the frequency of the current increases, so does the magnitude of the phase angle. The varying phase angle between load voltage and load current does not affect the PID position controller of the FTS system because the load current is directly proportional to the force exerted by the voice coil and normally in phase with the controller signal going into the amplifier.

In equation (3) v_L consists of the inductive voltage drop and the voltage drop across the resistors R_L and R_s . At 50Hz the load is still more resistive than inductive and the phase shift is relatively small. The power dissipation in the load with small or zero phase angle is calculated by

$$\begin{aligned} P &= V_{L,rms} I_{rms} \cos(\mathbf{f}) \\ &= \frac{V_L I}{2} \cos(\mathbf{f}) = \frac{12V \cdot 4.68A}{2} \cos(0) = 28W \end{aligned} \quad (5)$$

where $V_{L,rms}$ and I_{rms} are the root mean square values of the load voltage and load current respectively. This amount is also a ballpark value for specifying the power supplies needed.

4. Sensitivity of the amplifier due to modeling errors

A good amplifier design should be relatively insensitive and robust to parameter variations. The resistance R_L and the inductance L of the load have high uncertainties of ± 10 and ± 30 percent respectively and the gains introduced by the op amps may change some when the system ages. These parameter variations can be modeled as

unstructured additive uncertainties. Another source of errors arises from unmodeled plant dynamics. If ΔG denotes the difference between the actual plant G and the nominal modeled plant G^* then

$$G(s) = G^*(s) + \Delta G(s) \quad (6)$$

Figure 4 shows a simple open loop amplifier with a proportional controller $K(s)$, input voltage $V(s)$ and output current $I_L(s)$. The plant $G(s)$ represents the voice coil and amplification gains of the amplifier. In the open-loop configuration, the percentage error of the load current equals the percentage error of the model.

$$\frac{\Delta I_L(s)}{I_L^*(s)} = \frac{\Delta G(s)}{G^*(s)} \quad (7)$$

Equation (7) shows how sensitive the open-loop configuration is to modeling errors alone. If the modeling error is appreciable the resulting system output error might be unacceptably high. If information about I_L is fed back through a feedback gain H into the input terminal of the amplifier as indicated in figure 5, then the relationship between percentage output error and percentage modeling error is expressed by

$$\frac{\Delta I_L(s)}{I_L^*(s)} = \frac{1}{1 + H(s)G(s)K(s)} \cdot \frac{\Delta G(s)}{G^*(s)} \quad (8)$$

If the return difference $1+HGK$ were large, then a significant percentage error in modeling the plant would result only in a small percentage error in the output. Therefore, it is desired to maximize HGK in equation (8). It can be seen that with a feedback network installed, command following is less sensitive to modeling errors.

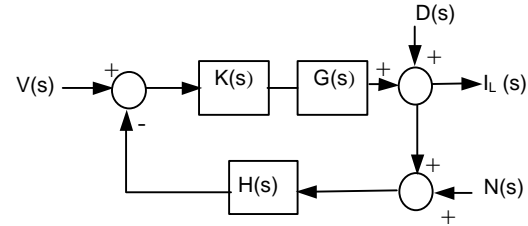


Figure 5: Closed loop amplifier with disturbance and noise

5. Disturbance rejection and noise response of the amplifier

The amplifier also has to be insensitive to internal noise N and compensate for external disturbances D as shown in figure 5. The expected disturbances are assumed to be low frequency signals representing mechanical input into the tool. Noise is generated in the circuit and is usually of high frequency. The output current I_L can be expressed in terms of input V , internal signal noise N , and external disturbances D by

$$I_L(s) = \frac{G(s)K(s)}{1 + H(s)G(s)K(s)} V(s) - \frac{H(s)G(s)K(s)}{1 + H(s)G(s)K(s)} N(s) + \frac{1}{1 + H(s)G(s)K(s)} D(s) \quad (9)$$

To investigate the influence of disturbances D on the amplifier assume that noise N and input V equal zero. Then I_L is related to D by

$$I_L(s) = \frac{1}{1 + H(s)G(s)K(s)} D(s) \quad (10)$$

For good disturbance rejection, the output I_L in equation (10) should be close to zero since the input V was assumed to be zero. This implies that the return difference $1+HGK$ has to be large at lower frequencies where the disturbances have their major energy content.

To analyze the effects of noise, assume that the disturbances D and the input voltage V are zero. From equation (9) the load current then equals

$$I_L(s) = -\frac{H(s)G(s)K(s)}{1 + H(s)G(s)K(s)} N(s) \quad (11)$$

Again, for good noise immunity the output I_L in equation (11) should be close to zero because the input was assumed to be zero. Since noise N is a signal with energy contents at high frequencies, the transfer function HGK has to be small at higher frequencies. Thus, the open-loop frequency response of the op amps used to build the amplifier should look like a low pass filter with high gain at low frequency and low gain at high frequency. Output

feedback in the amplifier is important to reduce the effects of noise and modeling errors as well as to increase command following properties.

6. Designing an integrator-type feedback controller

The amplifier's bandwidth is required to be higher than the open loop bandwidth of 160Hz determined by the voice coil. Two cascaded feedback networks are used to enhance the frequency response of the amplifier. A circuit diagram is given in figure 6 and represented in block diagram form in figure 7. The block diagram contains several transfer function blocks, which correspond to elements in the amplifier circuit. Table 1 summarizes the transfer functions of the various elements with a brief description.

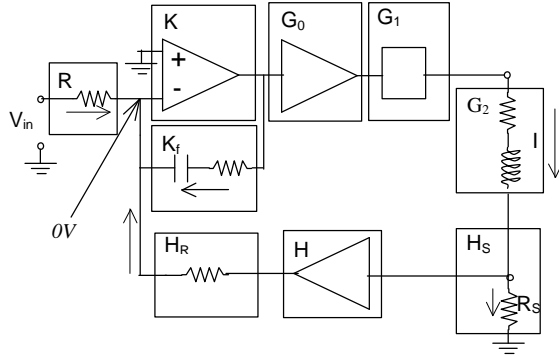


Figure 6: Circuit diagram divided up into TF blocks

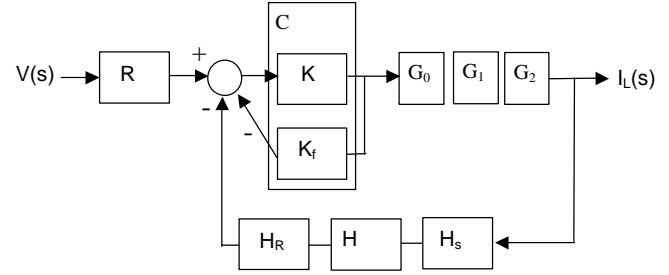


Figure 7: Block diagram representation of amplifier

Table 1: Transfer functions of various elements in the amplifier circuit

Name	Transfer function	Units	Description
R	$\frac{I_o}{V_i} = \frac{1}{5100}$	$\frac{A}{V}$	Input resistor of 5.1k Ω
K _{ol}	$\frac{V_o}{V_i} = \frac{76dB \cdot 12kHz}{s + 12kHz} = \frac{6310 \cdot 75400}{s + 75400}$	$\frac{V}{V}$	Open loop TF of power op amp used to build the controller (AD826). Open loop response taken from data sheet.
G ₀	$\frac{V_o}{V_i} = \frac{1.6 \cdot 12kHz}{s + 12kHz} = \frac{1.6 \cdot 75400}{s + 75400}$	$\frac{V}{V}$	Close loop TF of power op amp AD826 set to a gain of 1.6
G ₁	$\frac{V_o}{V_i} = \frac{7.5 \cdot 800000}{s + 800000}$	$\frac{V}{V}$	Closed loop TF of power op amp PA03 set to a gain of 7.5
G ₂	$\frac{I_L}{V_L} = \frac{1}{Ls + R} = \frac{1}{0.0025s + 2.4}$	$\frac{A}{V}$	TF of the load (voice coil)
K _f	$\frac{I_o}{V_i} = \frac{1}{R + 1/Cs} = \frac{Cs}{RCs + 1}$	$\frac{A}{V}$	TF of the inner feedback path. The values of R and C are to be determined by tuning the controller
H _R	$\frac{I_o}{V_i} = \frac{1}{5100}$	$\frac{A}{V}$	Resistor of 5.1k Ω in the outer feedback path after op amp
H	$\frac{V_o}{V_i} = \frac{20.8 \cdot 12kHz}{s + 12kHz} = \frac{20.8 \cdot 75400}{s + 75400}$	$\frac{V}{V}$	Gain introduced by an op amp (AD826) in the outer feedback path set to a gain of 20.8
H _S	$\frac{V_o}{I_L} = 0.02$	$\frac{V}{A}$	Sense resistor of 0.02 Ω to convert the load current into a voltage

The closed loop frequency response G_1 and the open loop frequency response A_{POL} of the PA03 are shown in figure 8. G_1 has a pole at about 800000 rad/s. Since the gain is 7.5, the closed loop frequency response of the power op amp G_1 is

$$G_1 = \frac{V_o}{V_i} = \frac{7.5 \cdot 800000}{s + 800000} \quad (12)$$

The open loop response of the AD826 is obtained the same way by noting that the open loop gain given in the data sheet is 76dB with a bandwidth of 12kHz. Hence, the open loop response can be expressed as

$$K_{ol} = \frac{V_o}{V_i} = \frac{76dB \cdot 12kHz}{s + 12kHz} = \frac{6310 \cdot 75400}{s + 75400} \quad (13)$$

These fast poles of the op amps could be neglected in the calculations and K_{ol} set to 6310V/V. R , H_s , and H_R are resistors that convert voltages into currents in the block diagram representation. At the summing point all currents sum to zero according to Kirchhoff's current law.

K and K_f in figure 7 can be combined to an equivalent block C containing a strictly proper third order transfer function. By selecting values for the resistor and capacitor contained in block K_f the amplifier can be tuned. The equivalent transfer function can be used to simulate the frequency response of the amplifier for different values of the capacitor and resistor in the integral-type feedback controller. Figure 9 shows an array of Bode plots for a constant capacitance of 0F and R ranging from 5kΩ to 500kΩ.

7. Frequency response measurements of the amplifier

The actual frequency response of the amplifier with no integral gain was measured with a signal analyzer. The frequency response was computed by dividing the cross spectrum between the input signal sequence and the output signal sequence by the power series spectrum of the input signal sequence. Therefore, the frequency response is a direct representation of the characteristics of the true system.

Figure 10 shows the frequency response of the amplifier/voice coil assembly resulting from a sinusoidal input voltage with amplitude 0.5V. Unfortunately, the maximum frequency of the measurements was limited by the bandwidth of the current probe that was used to measure the output of the amplifier.

There are still some discrepancies between the experimental and the theoretical models. Figure 10 shows some dynamics in the real system that have not yet been identified. For example, the dynamics at 48Hz are apparently caused by the first mode of the flexure that is attached to the voice coil. The bode plot shows the presence of multiple poles and zeros interacting with each other, as evidenced by the dip at 45 Hz, rise shortly thereafter (indicating a pole/zero pair), followed by a gentle -10 db/decade slope that begins to roll off further at 1 kHz. It is believed that the response will reach a -40 db/decade slope and -180 degree phase beyond 1 kHz, but the discrepancies are still being investigated.

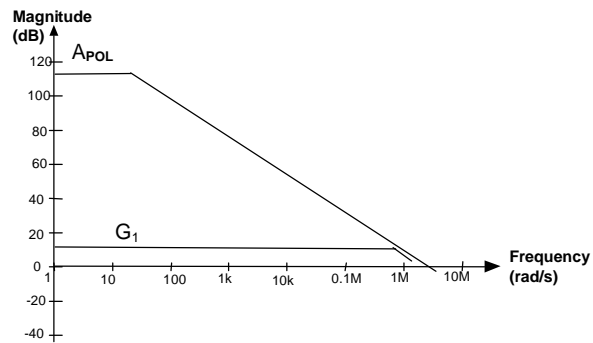


Figure 8: Open and closed loop response of the PA03

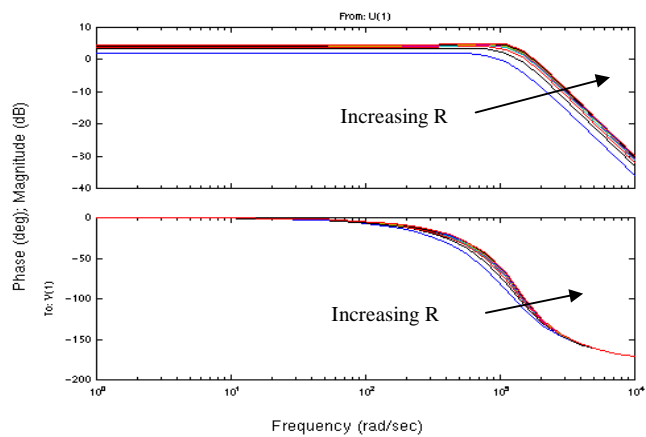


Figure 9: Response of the model for increasing R and C=0

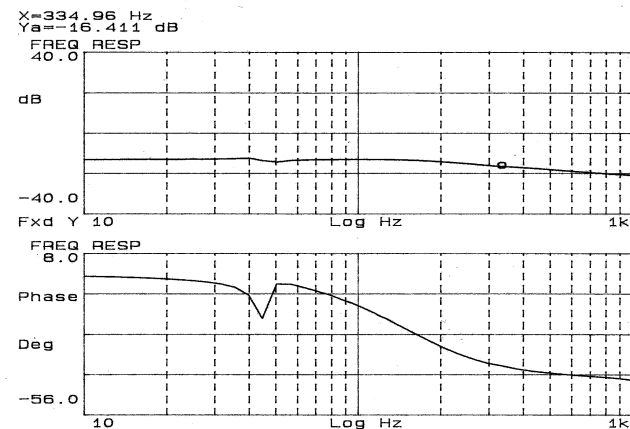


Figure 10: Frequency response of actual amplifier

8. Non-linearities

During the process of tuning the PID controller for the FTS system, the amplifier sometimes saturated because of very large and fast controller output signals. This means that the FTS system represents a difficult non-linear system. One possibility to describe non-linearities is to fit a higher order linear transfer function to non-linear frequency response data about some operating point. These transfer functions may be used to design the PID controller for the FTS system.

Matlab and Simulink were used to create an amplifier model (figure 11) that contains slew rate limits, saturation blocks, and back-emf (figure 12). The back-emf subsystem calculates the velocity of the flexure by differentiation of the displacement and a constant relationship between velocity and back-emf voltage generated. Virtual test inputs equivalent to those from the signal analyzer were fed into the model to calculate the frequency response in the linear region. Efforts are currently under way to verify the model.

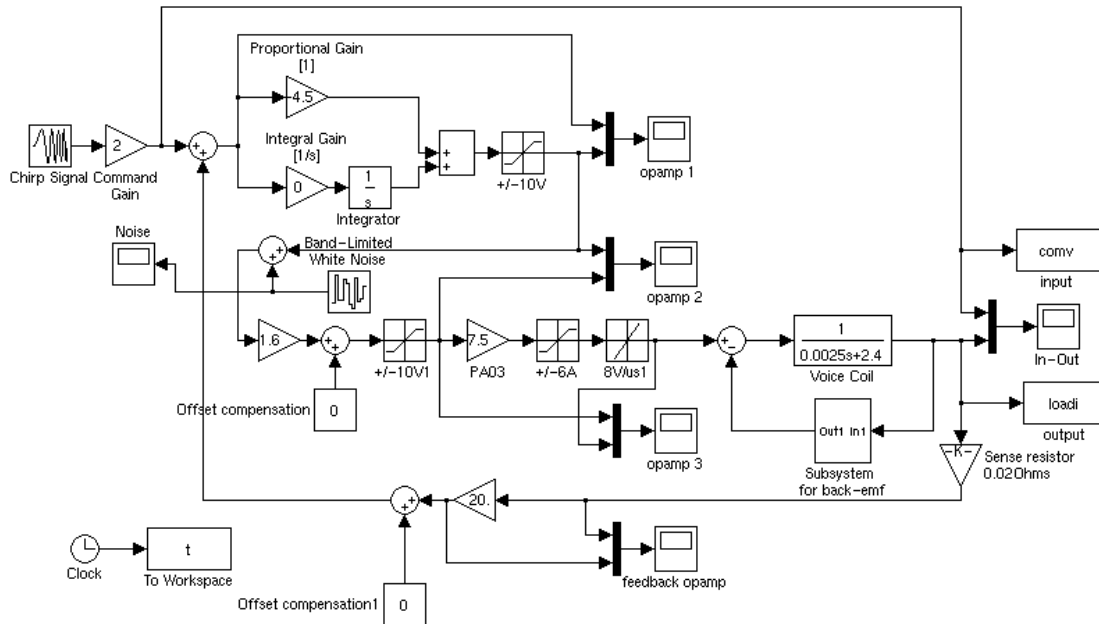


Figure 11: Simulink block diagram of actual amplifier

9. Conclusion

This work shows how techniques from classical control theory can be applied to design and analyze the performance of an amplifier for a precision motion mechanism utilizing a voice coil. It also points out many of the difficulties in getting the theory to accurately model the actual response. Work is continuing to identify the principal components required to develop accurate models of amplifiers used for precision applications.

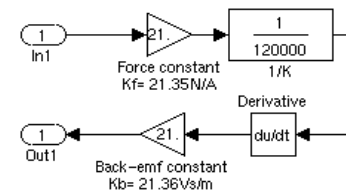


Figure 12: Back-emf subsystem for model

10. References

1. Zia A. Yamayee, Juan L. Bala, Jr., "Electromechanical Energy Devices and Power Systems", John Wiley & Sons, Inc., 1994
2. Richard C. Dorf, Robert H. Bishop, "Modern Control Systems", 7th edition, Addison Wesley, 1995
3. APEX Microtechnology catalog v8.5, Application notes, 1999
4. William J. Palm III, "Modeling, Analysis, and Control of Dynamic Systems", 2nd edition, John Wiley and sons, Inc